

Michael Schäferling · Stefan Nagl

## Optical technologies for the read out and quality control of DNA and protein microarrays

Received: 1 August 2005 / Revised: 2 November 2005 / Accepted: 13 January 2006 / Published online: 12 April 2006  
© Springer-Verlag 2006

**Abstract** Microarray formats have become an important tool for parallel (or multiplexed) monitoring of biomolecular interactions. Surface-immobilized probes like oligonucleotides, cDNA, proteins, or antibodies can be used for the screening of their complementary targets, covering different applications like gene or protein expression profiling, analysis of point mutations, or immunodiagnos- tics. Numerous reviews have appeared on this topic in recent years, documenting the intriguing progress of these miniaturized assay formats. Most of them highlight all aspects of microarray preparation, surface chemistry, and patterning, and try to give a systematic survey of the different kinds of applications of this new technique. This review places the emphasis on optical technologies for microarray analysis. As the fluorescent read out of microarrays is dominating the field, this topic will be the focus of the review. Basic principles of labeling and signal amplification techniques will be introduced. Recent developments in total internal reflection fluorescence, resonance energy transfer assays, and time-resolved imaging are addressed, as well as non-fluorescent imaging methods. Finally, some label-free detection modes are discussed, such as surface plasmon microscopy or ellipsometry, since these are particularly interesting for microarray development and quality control purposes.

**Keywords** DNA microarrays · Protein microarrays · Imaging · Fluorescent labels · Signal amplification

### Introduction

With the decoding of the entire genome of many organisms, the completion of the Human Genome Project, and the demand for high-throughput screening methods in pharmaceutical or biomedical research, new technologies for monitoring biomolecular interactions in high multi- plexity arose in the past decade. The basic tool for such screening experiments was the microwell plate, which has increasingly been replaced by microarray (or so-called biochip) formats because of their high degree of miniatur- ization. Specific instruments like automated nanodispens- ers and fluorescence scanner systems have helped to pave the way for many different applications of this new technology in recent years.

Most of the current biochip experiments focus on the investigation of DNA interactions to probe gene expression (e.g., by differential gene expression profiling), single nucleotide polymorphisms (SNPs) in individual genes, or on the identification of genetically modified food and seed. While the impact of DNA arrays will grow in functional genomics research and pharmagenomics, there is also an increasing trend to focus on the mapping of protein interactions. The determination of specific proteins among other regulatory elements is the key in understanding the regulation of various cellular mechanisms, and they can act as biomarkers for certain diseases in diagnostic applica- tions. This makes protein or antibody arrays promising tools for protein expression analysis, proteome research, medical diagnosis, detection of toxins in food and feed, and the discovery of binding domains of target molecules and receptors.

Since the development of in situ light-directed synthesis of oligonucleotides on glass surfaces [1] and the launch of high-density genome-wide DNA arrays by Affymetrix [2], glass substrates are dominating the microarray market. Now, activated glass slides coated by terminal functional- ized alkylsilane monolayers or polymeric binding matrices can be spotted with biomolecules by the end-user in any format and density. Many customized immobilization

M. Schäferling (✉) · S. Nagl  
Institute of Analytical Chemistry, Chemo- and Biosensors,  
University of Regensburg,  
93040 Regensburg, Germany  
e-mail: michael.schaeferling@chemie.uni-regensburg.de  
Tel.: +49-941-9434015  
Fax: +49-941-9434064

strategies are available for the attachment of biomolecules to all different kinds of microarray surfaces [2, 3].

Ready-made entire genome arrays from a large number of species, from arabisopsis to zebrafish, are commercially available on glass slides, representing transcripts of tens of thousands of different entire genes [4]. High-density protein microarrays were first prepared by Snyder et al. [5], providing a large fraction of the yeast proteome. The first human and yeast proteome microarrays are commercialized under the trade name ProtoArray [6].

The following overview highlights the current status of fluorescent read out methods for DNA and protein microarrays. To give a comprehensive picture of this topic, new developments in fluorophore excitation like total internal reflection fluorescence (TIRF), in binding detection, e.g., by Förster resonance energy transfer (FRET) or fluorescence lifetime imaging (FLIM), will also be considered in addition to the commonly used laser scanners or fluorescence imaging systems. To complement this subject, non-fluorescent and label-free methods, like surface plasmon resonance (SPR) and ellipsometry, will be touched on, since these have found particular interest with respect to quality control issues for microarray fabrication.

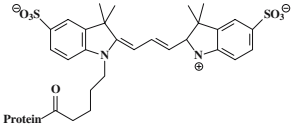
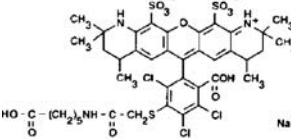
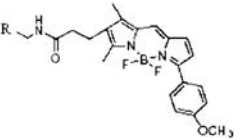
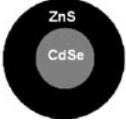

## Fluorescent labeling and detection of biomolecules

Direct labeling of a biomolecule involves the introduction of a covalently linked fluorophore into the nucleic acid sequence or the amino acid sequence of a protein or antibody. Fluorescein, rhodamine derivatives, the Alexa and BODIPY dyes [7], and the cyanine dyes [8] are widely used labels. The optical properties of typical dyes used for microarray experiments have already been reviewed in detail, including problems like photobleaching and quenching effects after bioconjugation [9]. Structures and optical properties of frequently used fluorescent labels are given in Table 1.

### Nucleic acid labels

The covalent labeling of target DNA molecules is usually integrated into the PCR (polymerase chain reaction) process. Fluorophores linked to uridine-5'-triphosphates are available for the enzymatically mediated statistic insertion into the nucleotide sequence (random primed labeling technique) [10, 11]. Alternatively, such labeled

**Table 1** Structures and optical properties of frequently used fluorescent labels in DNA and protein microarray technology

Dye	Structure	Absorption/Emission Maxima
Cy3		$\lambda_{\text{abs}} = 552 \text{ nm}$ $\lambda_{\text{em}} = 570 \text{ nm}$
Alexa 546		$\lambda_{\text{abs}} = 546 \text{ nm}$ $\lambda_{\text{em}} = 580 \text{ nm}$
Bodipy TMR		$\lambda_{\text{abs}} = 542 \text{ nm}$ $\lambda_{\text{em}} = 574 \text{ nm}$
QDot 605		$\lambda_{\text{abs}} \propto 1/a^*$ $\lambda_{\text{em}} = 605 \text{ nm}$
R-phycoerythrin		$\lambda_{\text{abs}} = 565 \text{ nm}$ $\lambda_{\text{em}} = 578 \text{ nm}$

\* increasing absorption coefficient with decreasing excitation wavelength

triphosphates can be coupled to the 3'-terminus of DNA strands by the enzyme terminal transferase [12]. A typical gene expression profiling experiment applying a competitive assay method is illustrated in Fig. 1. Two fluorophores are used, which exhibit different excitation and emission wavelengths but similar fluorescence intensities, for example, the cyanine dyes Cy3 and Cy5 (excitation maxima at 548 nm and 646 nm, respectively).

Several methods are available for a secondary (or indirect) labeling of the target DNAs that are captured on the array by hybridization. These include the use of amino allyl-modified cDNAs, which can be labeled by amino-reactive dyes (active esters) or the incorporation of nucleotides which are linked to biotin or haptens and can be detected by fluorescently labeled streptavidin or antibodies [7]. The combination of secondary labeling with signal amplification methods will be discussed later. Labeling techniques using DNA intercalators have not found extension to microarray experiments yet and therefore they will not be discussed within this review.

### Protein stains

Owing to the range of different applications of protein microarrays, many different ways for performing the fluorescence analysis of such arrays have been described in the literature. The arrangement of protein assays on microarray surfaces are reviewed in numerous articles [13] and textbooks [14]. Capture probes can be antibodies, peptides, proteins, haptens, or aptamers (see Fig. 2), which are immobilized either electrostatically, covalently, or by metal-chelate interactions (e.g., Ni-coated surfaces which bind selectively to proteins expressed with His-Tags).

To simplify matters, two different kinds of applications of protein microarrays can be distinguished [15]:

- (1) expression profiling: this includes phenotyping of cells, detection of disease markers, and differential diagnosis or profiling of infectious diseases, allergies, or autoimmune diseases
- (2) interaction profiling: mapping of interactions between protein domains, identification of enzyme regulators, drug screening, and specific immunoassays.

Direct labeling of target proteins or secondary antibodies in sandwich-type assays can be achieved by amino-reactive dyes in the form of their active ester or isothiocyanate derivatives. Thiol-reactive dyes (maleimide, iodoacetamide, or disulfide derivatives) for a specific coupling to cysteine units are also available, as well as hydrazides for labeling aldehyde groups of polysaccharide subunits in glycoproteins [7]. Fusion proteins are often used for interaction-profiling-type experiments. Protein samples can be cloned (or subsequently modified) with tags like GST (glutathione S-transferase) or biotin for protein-protein interaction studies. The binding on the microarray can be probed by labeled anti-GST or streptavidin, respectively [5, 16].

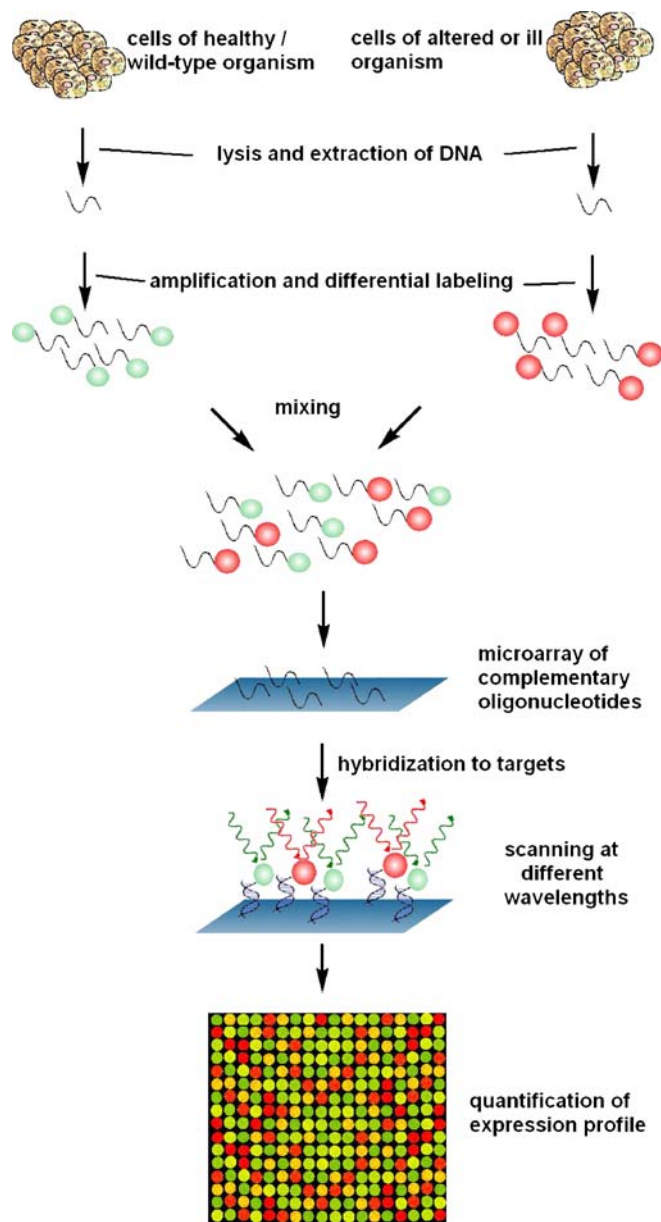


**Fig. 1** Differential gene expression profiling: PCR-amplified cDNAs from sample A (labeled with a red fluorescent dye) and reference B (labeled with a green fluorescent dye) are incubated competitively on an oligonucleotide microarray. The read out of the array is performed at two different wavelengths according to the applied dyes. A pseudocolor image visualizes the ratio of the hybridized samples on each spot

In addition to organic dyes, which are the dominant detector molecules used for the purpose of microarray screening, fluorescent proteins are well-suited labels for biomacromolecules. R-Phycoerythrin (RPE) is one prominent example, a phycobiliprotein exhibiting a high quantum yield, absorption cross-section, and water solubility. Compared to organic dyes, it showed improved signal intensities on the read out of protein microarrays, using antibodies as capture probes. The intensities are compar-

## Protein Microarrays

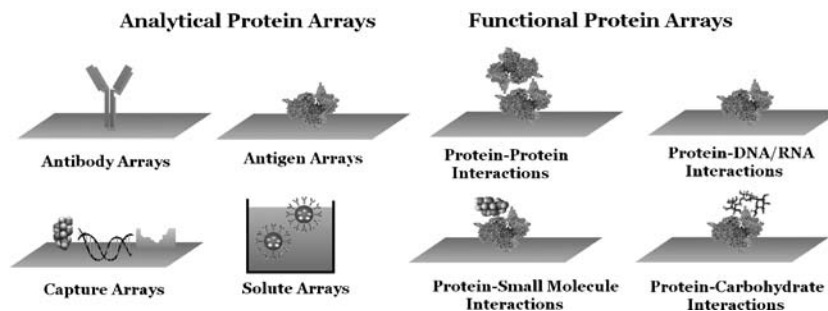


**Fig. 2** Typical types of protein microarrays, divided into two subcategories. Analytical protein arrays (*left*) are used for quantification of target analytes, e.g., antigens using antibody arrays or antibodies using antigen arrays (*top*). Proteins of interest can also be captured using small molecules, aptamers, or molecularly imprinted

polymers. Alternatively, surface-functionalized nanoparticles may be used in solute arrays (*bottom*). Functional protein arrays (*right*) can detect interactions of immobilized proteins with virtually any kind of natural or artificial compound, but only the most common are shown

able to those of nanoparticles (see next section) [17]. RPE conjugated to streptavidin or several antibodies is commercially available [7]. Streptavidin conjugates can also be used as labels in DNA [18] or peptide nucleic acid (PNA) [19] microarrays.

Proteins can be expressed conjugated to a kind of fluorescent protein based on the green fluorescent protein (GFP) by genetic engineering. By variation of the chromophore system, different fluorescent proteins can now be engineered with emission wavelengths spanning the whole visible range, e.g., a yellow fluorescent protein or a red fluorescent protein (DsRed). Their luminescence intensities are far below the commonly used organic dyes. Nevertheless, they have been used for protein interaction screening [20] and protein expression profiling [21] with the help of microarray formats. GFP can even be expressed with a specific DNA binding domain and can therefore be used as a marker for DNA arrays [22].

### Nanoparticles

Organic dyes are the most common and versatile stains to date, but they are associated with inherent problems, e.g., the interference of their spectral properties with the environment. Oxygen quenching, pH sensitivity, and changes of the excitation and emission wavelengths and quantum yields after conjugation to proteins can be observed [23]. The number of dyes which can be attached to a biomolecule is limited. Therefore, the amount of fluorophores bound to the microarray surface is very low. This necessitates narrow optical bandpass filters for background suppression and high light intensities, which is a major problem because most organic dyes tend to photobleach. Three main types of fluorescent nanoparticles have been developed, which may overcome these limitations.

*Polymeric nanoparticles* (frequently termed nanobeads or nanospheres) have been doped with fluorescent dyes for bioimaging applications [24, 25] and for immunoassays [26]. Consequently, they have also entered the microarray

field [17]. The predominant materials for the preparation of nanobeads, which are commercially available, are polystyrene (“latex”) [26, 27], poly(acrylonitrile) [28, 29], or poly(methylmethacrylate) [30, 31] and derivatives like poly(decyl methacrylate) [32]. Their synthesis via emulsion polymerization yields highly monodisperse particles, with diameters from 20 nm to several  $\mu\text{m}$ , according to reaction conditions. Bioconjugatibility can be achieved by addition of a co-monomer containing free carboxy groups. The beads can be doped with lipophilic dyes, which can be incorporated during synthesis or subsequently by swelling in organic solvents. These nanospheres can contain thousands of dye molecules yielding extremely strong fluorescence. Furthermore, phosphorescent dyes can be included, which facilitates time-resolved fluorescent detection and imaging and time-resolved resonance energy transfer (TR-FRET) assays [33]. Incorporation into polymer matrices leads to a structural rigidization of the dye and a shielding from quencher molecules, which is often accompanied by an increased quantum yield. Indeed, high signal intensities could be obtained with nanoparticle-streptavidin conjugates as labels for protein microarrays, but they also showed a high background [17]. This unspecific binding to the surface occurs presumably due to their inherent tendency for agglomeration and precipitation—a major drawback for the use of polymeric nanobeads as labels.

Luminescent nanospheres for bioconjugation can alternatively be prepared on *silica particles* and used as labels for DNA and protein microarray analysis [34]. The hydrophilicity of the silica structure avoids precipitation problems in aqueous solutions. They are usually synthesized using a water-in-oil microemulsion method [35]. Water-soluble fluorescent [36] and phosphorescent complexes of ruthenium [34, 35], europium [37], or terbium [38] can be encapsulated into the silica network. Terminal-functionalized alkyl silanes can be incorporated during synthesis, providing binding sites for biomolecules. Monodisperse particles of 70-nm diameter containing the phosphorescent dye tris-(2,2'-bipyridyl)-ruthenium showed a signal intensity 39 times higher than that of quantum dots

(see next section), 1,290 times higher than that of the commercially available Texas Red label, and 72,000 times higher than that of the pristine label on comparative microarray trials [34].

Nanocrystals prepared from semiconductor materials are called *quantum dots* (QDs). They are spherical in shape, with core sizes typically between 2 and 10 nm, and can be coated with biocompatible surfaces [39–41]. At this size scale, quantum effects determine the optical and electronic properties. The energy gap between valence and conduction band increases with decreasing size, which affects the emission wavelength. Thus, the emission spectrum can be tuned by the choice of material and the size of the nanocrystal. They can be excited at virtually any wavelength shorter than 550 nm. Commercially available QDs are composed of CdSe, among other materials like CdTe, CdS, ZnSe, and InAs, and can be engineered with different particle sizes to yield emission at different wavelengths over the entire visible range [42]. The luminescent core is passivated by epitaxial growth of a thin surface-coating layer, which consists of a material with a higher band gap (e.g., ZnS or CdS). This is associated with a dramatic increase in quantum yields. Other merits of core-shell nanomaterials are their insensitivity towards environmental interferences and photobleaching, and their narrow emission spectra. Water solubility can be provided by silane or thiol surface chemistry. Reactive functional groups, including primary amines, carboxylic acids, alcohols, and thiols, can be applied to the surface, which can be then be covalently conjugated to a variety of biomolecules [43]. Such conjugates (which are capable of biomolecular recognition) have found numerous applications in biotechnology, in vivo imaging, and the detection of multiplexed bioassays [44–47].

In a groundbreaking study, QDs have been used as labels on cDNA microarrays for the detection of single nucleotide polymorphisms [48]. Subsequently, QD–streptavidin conjugates served as detectors for biotinylated micro-RNAs captured on cDNA microarrays [49]. Owing to their advantageous optical properties, it is not surprising that QDs have also forged ahead as labels for protein and

antibody microarrays, e.g., for the detection of toxins [50] and signal protein profiling [51]. As most microarray readers are equipped with excitation sources like green and red lasers aligned for the detection of Cy3/Cy5 or the equivalent Alexa dyes, they do not fit the requirements for the excitation of quantum dots, which can be more efficiently excited at wavelengths shorter than 530 nm. Another unsolved problem which appears with QDs is the non-specific absorption on the surface and the resulting high background signals.

### Signal amplification

It is quite obvious that the binding of labeled biomolecules on a surface yields only very weak fluorescence. Analyte concentrations are generally low and the density of adsorbed biomolecules on a 2D monolayer-coated surface is limited. Chip surfaces coated with 3D polymer networks like hydrogels, nylon or nitrocellulose membranes, and polymer brushes provide a larger surface area and therefore a higher probe density, which results in higher fluorescence signals. But this is accompanied by higher background signals due to non-specific adsorption, and the diffusion of the target molecules to the immobilized recognition sites is restricted.

In the case of DNA arrays, the analyte concentration itself can be multiplied by the PCR reaction or related *target amplification* techniques [52]. Target amplification approaches, which can easily be adapted on microarray formats, are the rolling circle amplification (RCA, Fig. 3) method and the ligase chain reaction. The applicability of both methods on DNA arrays has been demonstrated for genotyping and SNP detection [53–55].

In immunodiagnosics, the enzyme-linked immunosorbent assay (ELISA) is a widespread method applied in microwell plates, which makes use of enzymatic *signal amplification*. Detection of proteins (antibodies, antigens, toxins) is achieved by a specific secondary antibody, usually in a sandwich-type assay (Fig. 4). This detector antibody is conjugated to an enzyme which can generate a

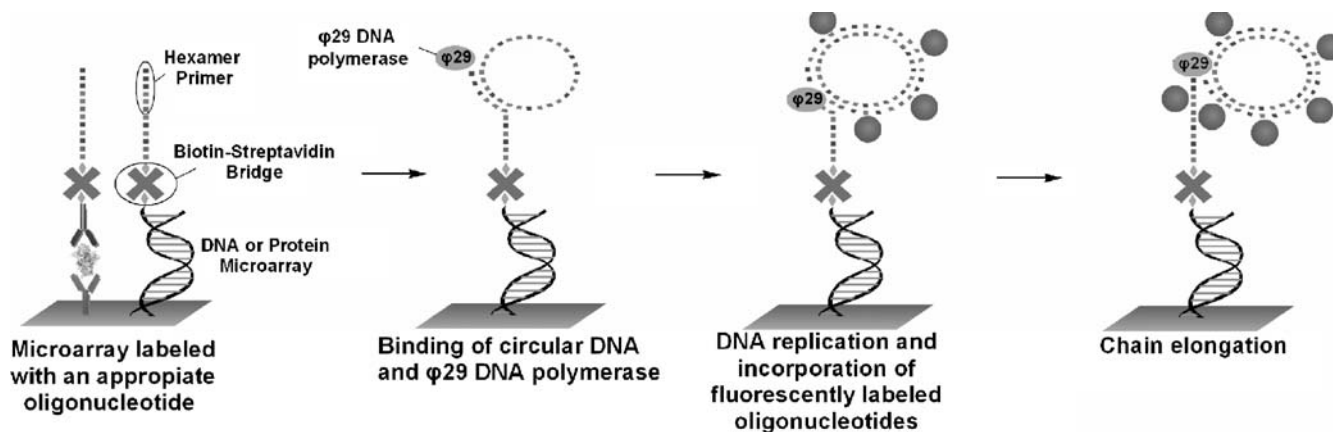


**Fig. 3** Principle of RCA (rolling circle amplification) on microarray formats. Starting from a circular DNA matrix, a multiple labeled sequence is generated at the positions where the primer is present

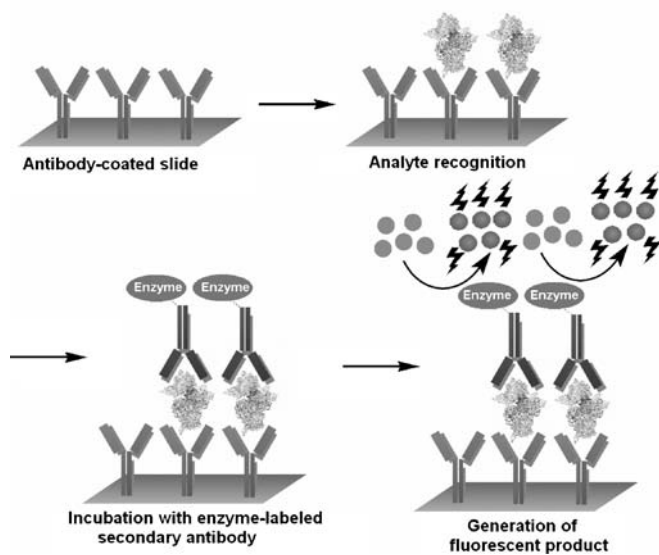
large number of colored (or fluorescent) product molecules from non- or weakly colored (or non-fluorescent) indicator molecules. Two types of enzymes are commonly used for ELISAs: alkaline phosphatase (AP) or horseradish peroxidase (HRP) [56]. The latter can also be used for chemiluminescent detection schemes, which are highly sensitive, e.g., the oxidation of luminol [57]. Phosphatases convert a non-fluorescent organic phosphate into a fluorescent product through dephosphorylation (Table 2). Generally, direct binding tests and competitive assays can be performed in this manner.

Only a few efforts have been made to transfer ELISAs to the microarray format. Laser scanner systems (see next section) can usually locate a high excitation intensity on a small area of the microarray surface, so fluorescently labeled secondary antibodies can be used without the need for enzyme conjugation and signal amplification. The lack of microwells on planar biochip substrates makes a parallel screening of different analytes with ELISAs difficult, because the entire chip can usually be exposed to only one analyte at a time. The first antigen arrays for detection of different monoclonal antibodies were presented by Mendoza et al. [58] In this study, glass slides coated with a Teflon matrix, which leaves 96 individual addressable cavities, were used; this was therefore a compromise between microwell plates and 2D microarrays. An array of 144 microspot elements was printed in each cavity. Antibody binding events were detected by a substrate which forms fluorescent precipitates in the presence of AP. Several applications have since been reported using AP-based fluorescent ELISAs for protein profiling and screening on microarray formats [59, 60].

Peroxidase conjugates for chemiluminescent antibody detection on microarrays were introduced by Joos et al. [61] Chemiluminescent systems have been used for the simultaneous detection of multiple cytokines in patient sera

[62] or various antibiotics in milk [63]. The tyramide signal amplification technique, sometimes called CARD (catalyzed reporter deposition), has also proven useful for microarray applications, e.g., for the detection of allergen-specific antibodies [64] or growth factors [65]. It is an HRP-mediated detection method that utilizes its catalytic activity to generate high-density labeling of a target protein at the tyrosine units with tyramide derivatives of fluorescent dyes. The CARD method has even been transferred to DNA arrays and showed improved sensitivity compared to directly labeled target molecules [66]. Generally, the use of hapten-modified (or biotinylated) PCR products allows ELISAs to be used for the read out of DNA arrays [67]. Vice versa, the RCA method can be applied to protein arrays, if the antibody detector is labeled with an appropriate oligonucleotide primer [68].

A signal amplification can also be achieved by modifications of the microarray surface itself. One method is surface-enhanced fluorescence in which the absorption and emission of a fluorophore is enhanced at a certain distance from a metal resonant layer or a metal nanoparticle [69]. The signal intensities can be improved several times by using gold nanoparticles as additional labels to organic dyes in a target mixture with a ratio of 1:2, respectively [70]. Another approach for signal enhancement is the application of highly reflective coatings by incorporation of highly refractive nanostructured TiO<sub>2</sub> particles into low-refractive surface matrices (polymers or amorphous silica prepared by the sol-gel technique) [70, 71]. In a comparative study, the screening results on 11 different kinds of array surfaces, including polymer gel and silane-coated glass slides, were reported. All important advantages of a microarray experiment are illustrated by applying five different monoclonal antibodies in a 20×18 spot matrix: ease of chip preparation and handling, storage, signal intensities, reproducibility, and detection limits. Based on these investigations, highly reflective slides with a mirror-like surface coating were found to provide high spot uniformity and reproducibility [72].

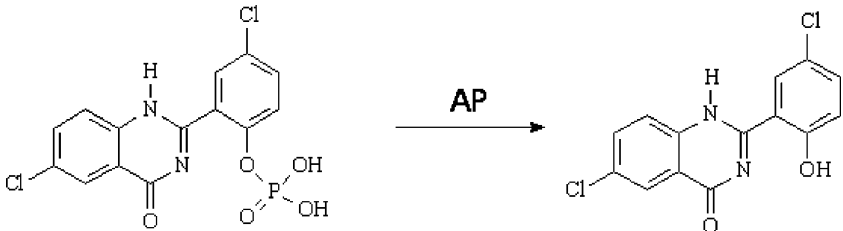
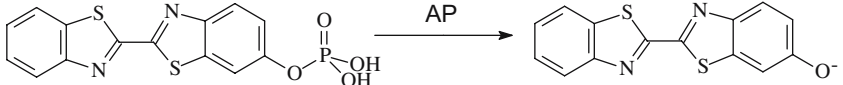
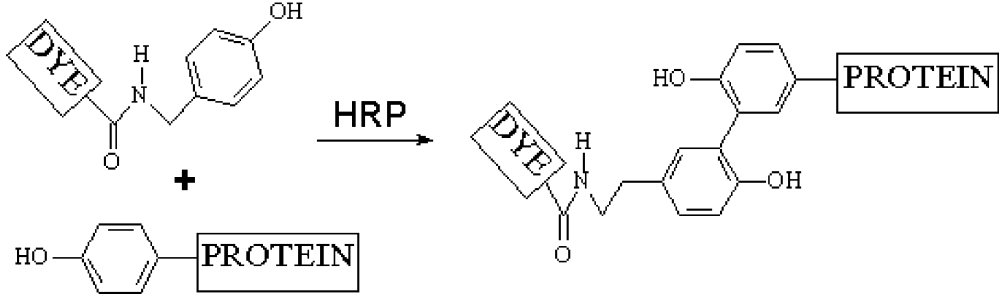
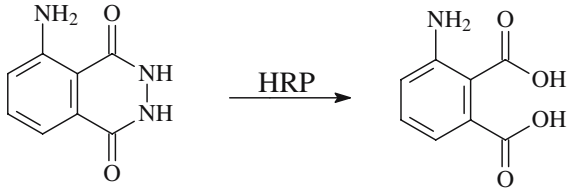


**Fig. 4** Illustration of a fluorescent sandwich ELISA. Alkaline phosphatase or horseradish peroxidase are the preferentially applied enzymes

### Laser scanner versus imaging instruments

Image-based screening is particularly interesting in pharmaceutical high-throughput drug discovery [73]. In vitro assays carried out in microwell plates are usually analyzed by non-imaging microplate readers. The read out is done well by well at fixed positions, so each well is considered as a homogeneous point source. The plate has to be moved between the punctiform light source and the detector. Image-based screening now creates a digital image of the whole plate, e.g., with a CCD (charge coupled device) camera as detector, which localizes multiple data points (pixels) within each target area. Therefore, the advantage of imaging is speed and high resolution. Imagers can detect multiple wells simultaneously and in short intervals, which is advantageous for kinetic assays. Finally, subcellular resolution can be achieved in cell-based screening in combination with automated microscopy systems.

**Table 2** Fluorescent and chemiluminescent detection methods for ELISAs and the tyramide signal amplification technique

Dye	Enzymatic Reaction	Absorption/ Emission
ELF-97 [14]		$\lambda_{\text{abs}} = 360 \text{ nm}$ $\lambda_{\text{em}} = 530 \text{ nm}$
AttoPhos [64]		$\lambda_{\text{abs}} = 440 \text{ nm}$ $\lambda_{\text{em}} = 575 \text{ nm}$
Tyramide [14]		depends on applied label
Luminol		Chemiluminescence $\lambda_{\text{em}} = 445 \text{ nm}$

AP = alkaline phosphatase, HRP = horseradish peroxidase

In the case of well-free array formats, two alternative concepts of microarray fluorescence readers have become widely accepted: laser scanner and imaging systems. Typically, *scanners* are equipped with one to three lasers with different wavelengths, a movable x/y stage, and a photomultiplier tube (PMT) as detector (Fig. 5). A PMT is based on a photocathode combined with an amplification of the emission electrons in dynode chains. Array *imaging systems* are originally based on gel or blot documentation stations and make use of a CCD camera as detector and a white light source equipped with an appropriate set of optical filters or an array of light-emitting diodes (LEDs) in combination with fiber optic waveguides for the excitation of the fluorophores. Appropriate white light sources include halogen lamps or xenon arc discharge lamps, which show a fairly homogeneous intensity distribution over the visible range. In general, a laser scanner is used to evaluate the array pixel by pixel while it is moved in the optical path between light source and PMT. Imaging systems can detect the whole array at once by use of an area detector, most commonly a CCD or CMOS chip. Within this review, the term imaging is exclusively used only for simultaneous area measurements, as just described. Note, however, that the term imaging is often also used in a

broader sense, referring to the procedure of creating an image of a certain area. In this context, imaging systems also include point-by-point scanning detectors.

Scanners with various lasers can screen dual-fluorophore samples either sequentially or simultaneously, which is an important feature for differential gene expression analysis, but makes this kind of instrument rather expensive. Lasers provide monochromatic and collimated light. Besides gas lasers, e.g., Ar ( $\lambda=488, 514 \text{ nm}$ ) or He/Ne ( $\lambda=633 \text{ nm}$ ), semiconductor (diode) lasers are preferentially installed in

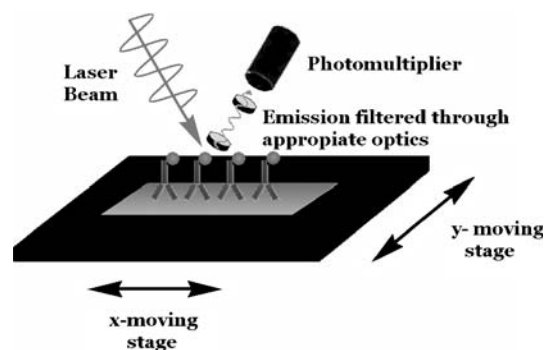


**Fig. 5** Components of a laser scanner system

microarray scanning systems (e.g., InGaP or AlGaInP), which can be tuned over a broad wavelength spectrum in the red (630–750 nm). The laser beam scans the sample, dwelling on each position (pixel) for some microseconds.

Stationary CCD-based imagers can cover a large area, adjustable by different lenses, so that one slide can be imaged at once. The white light source (or LED array) has to illuminate the whole sample area, providing much lower power densities. The number of pixels is predetermined by the CCD chip, which can integrate the emission signals in a timeframe of seconds to collect enough light to create a meaningful image. The great advantage of a scanner system is that a laser beam can focus more energy on a small area to excite fluorophores, and thus they collect more light in less time. They therefore have generally a higher sensitivity and shorter signal integration times than CCD-based systems. However, this higher output is not essential, since fluorophores can reach a saturation point at which further excitation leads to intense photobleaching and non-linear emission response. Imaging systems can easily be equipped with an assortment of appropriate filters for different excitation wavelengths. This makes them to versatile and, compared to scanners, low-cost instruments.

The scanner set-ups clearly dominate the reader market, especially for high-density arrays, which are required in expression profiling, because of their higher lateral resolutions. CCD detectors are limited by the number of pixels on the chip, which is usually in the range of  $10^6$  (e.g.,  $1,024 \times 1,024$  pixel with a size around  $10 \mu\text{m}^2$ ). The linear (or dynamic) range of a CCD detector is specified as the ratio of the capacity of each spot on the CCD array to the read out noise level. Furthermore, a CCD detector responds linearly to increasing integration times. As a matter of course, dark current (random electrons circulating in the device in the absence of light) also increases proportionally with exposure and increases the noise level. The dynamic range of a CCD chip is 14 to 16 bit, so at least  $10^4$  grey levels can be distinguished. This is comparable to the composite dynamic range of a PMT with analog-to-digital converter. Generally, the linear range of a PMT is defined as the difference in current between the noise level and the highest gain setting. The signal output from a PMT (typically in a range of 10 nA to 100  $\mu\text{A}$ ) is converted to a 16-bit digital value, the equivalent of  $2^{16}$  (=65,535 or about 4.5 orders of magnitude) distinguishable intensity values. This definitely covers the dynamic range of fluorescent bioassays or screening experiments. Another important parameter is the quantum efficiency (QE), a term which is defined as the emitted electronic signal of the detector device relative to the received incoming photon signal. Generally, CCDs have about a twofold greater QE than standard PMTs. For a more detailed discussion on the characteristics of the different detector systems see ref. [74].

Several articles compare commercially available microarray readers and discuss their instrumental progress [75, 76]. A summary of the most widely used platforms can also be found on the internet (e.g., at [biocompare.com](http://biocompare.com) [77]). The systems described above are arranged as an epi-

fluorescence set-up, based on a reflected (episcopic) pathway of excitation light and the light emitted by the fluorophores. Consequently, nontransparent array substrates may be used as well as glass substrates. In laser scanner instruments, the excitation light is usually reflected by a dichromatic mirror (beamsplitter) before it impinges the microarray slide. This dichroic mirror acts as a long-pass filter. It reflects the excitation light to the array slide but is transparent for higher wavelength light, such as the Stokes-shifted emission of the fluorophores absorbed on the array, which is directed to the detector. The main advantage of this set-up is the elimination of noise caused by stray light from the microarray surface. This is a major problem using organic fluorophores with their narrow Stokes shifts, as the excitation light is many magnitudes stronger than the emitted light. Moreover, it has to be kept in mind that only a small fraction of the photons emitted from a fluorophore on the array surface will hit the detector.

Another development in microarray read out, adapted from fluorescence microscopy devices for imaging of tissue samples, is the use of a confocal configuration. In this case the laser excitation light and the emitted light are channeled through pinholes, which are adjusted to the focal points of a lens. Consequently, the excitation light is focused on a small area and the emission light which is out of focus is rejected. The focus typically can be varied from a few hundred nanometers to a few micrometers. This set-up effectively separates light only from a certain plane. This leads to improved signal-to-noise ratios, as only the fluorescence proximate to the slide interface is of analytical significance. The demands of this technique are therefore a very flat surface on the microarray spots, which is in practice a major problem, and a sufficient scanning speed to avoid photobleaching of the fluorophores. The necessity for confocal imaging in microarray scanning is discussed controversially in the literature, as most of the background comes from unspecific binding of labeled biomolecules to the slide surface, which occurs in the same plane of focus as the sample [74].

Another important point for the lab user is the image analysis and evaluation software. A huge number of software packages with different features, primarily developed for DNA array analysis (e.g., image processing, superimposition of dual wavelength scans, automated spot recognition, and elimination of bad spots, statistical analysis) are available. An extensive compilation can be accessed via the internet, including links to the manufacturers and downloads of free demos [78]. Regarding the evaluation of the whole read out system performance, some important parameters should be considered:

1. *Robustness of calibration procedures.* It has to ensure reproducibility of the results over time.
2. *Detection limit.* It specifies the weakest signal the system can quantify reliably and is calculated for imaging applications as SNR (signal-to-noise ratio), with  $\text{SNR} = (\text{signal} - \text{noise}) / (\text{standard deviation of noise})$ . The minimum signal that can be accurately quantified is commonly considered for a SNR of 3.



Evaluation software postulates a SNR higher than 10 for a reliable microarray analysis and quality assurance.

3. *Field uniformity.* A uniform excitation and imaging field has to guarantee that different areas of the microarray slide give comparable data.
4. *Reproducibility.* This universal parameter in the analytical sciences accounts for reproducibility of signal outputs from a microarray imaging system including scan-to-scan reproducibility and the equality of signal intensities from different spots with identical samples on the same slide. Instrumental claims like operation conditions and warm-up and stabilization times of detectors and light sources have to be considered to ensure reproducibility.

Besides these instrumental features, there are some more significant parameters which are affected by the accuracy of the microarray preparation:

1. *Spot-to-spot variation.* Spots with identical loading have to give the same averaged signal. Besides instrumental features, variations can be caused by deficient pipetting and spotting.
2. *Spot homogeneity.* A high variation of signal intensities within one spot (feature) complicates a reliable analysis. Doughnut-shaped features are a perseverative artefact in microarray experiments. The homogeneity is usually expressed as coefficient of variation (CV), that is the ratio between the standard deviation of all pixel intensities within one spot and the mean intensity as a percentage. The CV should not exceed a value of 20%.
3. *Background variation.* A high standard deviation of the background can cause problems in discriminating actual spot features from regions with random high background. The standard deviation from the background of the entire chip area divided by the mean value of the background intensity should also be less than 0.2.
4. *Signal-to-background ratio.* This is probably the most important parameter and has to be calculated for every single spot to assess its significance as a ratio between the average intensity from the spot and the average background intensity. To be confident that the spots are clearly differentiable from the background, evaluation software programs propose a ratio larger than 10 for quality assurance.
5. *Saturated pixels.* Pixels with signal intensities higher than the dynamic range of the detector adulterate the statistical spot evaluation. Their amount should not exceed 1%, otherwise a rescan with lower PMT gain or CCD exposure time is appropriate.

These quality control quantities are the basis for a comparable microarray analysis. Issues of quality control management become increasingly important for routine microarray applications [79, 80]. Standardization of microarray preparation protocols, the use of robust calibration procedures with stable fluorescent standards, and the normalization of the data with respect to the key

parameters listed above are important matters for a better interpretation of data from different laboratories. The generation of consistent, verifiable results is still difficult because of the lack of standards to validate these analyses. A consortium of the American National Institute of Standards and Technology (NIST) and scientists from industry started to work on the design of reference materials and test standards for gene expression profiling [81], while other groups are also currently aiming to develop microarray standards [82].

---

### Current progress in photodetector arrays

Active-pixel image sensors based on complementary metal oxide semiconductor devices (CMOS) are a less expensive alternative to CCD cameras, and can lead to more compact and portable instruments [83]. In principle, CMOS detectors represent an array of lateral bipolar phototransistors operating at a lower power supply than CCDs. However, CMOS technology has two principle disadvantages, which have to be overcome in the near future if it has to compete with CCDs: first, the stationary noise pattern is higher than that found in a CCD; and second, each pixel contains a photo diode and, in addition, amplifiers and selection circuitry, so that the actual area of the pixel that gathers photons is smaller. This is reflected in a reduction in sensitivity in comparison to a similarly sized CCD. For low lateral resolution applications, CMOS detectors may replace CCDs in the near future.

A strong impact on the development of sensitive detection methods arises from single-photon counting modules (SPCM). This technology is based on avalanche photodiodes, which are semiconductor junctions operated under a reversed bias voltage. A charge-free depletion region is thus created, which behaves as an insulator, so that almost no current flows through the device. Under these conditions, a large electric field can be applied which accelerates electrons generated inside the material (e.g., by single photons) by the so-called process of impact ionization [84, 85]. This method can be combined with confocal microscopes or fluorescence correlation spectroscopy and can measure the fluorescence emitted by analytes in the zeptomole range down to single molecules. Furthermore, it is possible to acquire multiple measurements simultaneously with a multichannel SPCM array. This makes SPCM useful for multi-wavelength systems or the parallel collection of different parameters, such as fluorescence intensity, molecule diffusion times, fluorescence lifetimes, and fluorescence polarization. SPCM could also enable fluorescence detection for high-throughput screening instrumentation, using the corresponding optics for a consecutive or a simultaneous measurement of the sample spots on a microarray. Applications in related systems like microfluidic devices have also been demonstrated [85].

The lifetime-based imaging of sensor arrays, as presented in below in "Time-resolved fluorescence", is exclusively performed in the time domain. Nevertheless, phase-sensitive detection systems in the frequency domain

exhibit an interesting option by using multichannel photomultiplier tubes for the scanning of biosensor arrays [86].

### Advanced fluorescence excitation and detection technologies

Besides the standard microarray read out methods described in the last section, which are based on steady-state measurements of the emitted fluorescence intensity by means of an epi-configuration, several new approaches have been elaborated during recent years, starting from new methods for fluorophore excitation, time-resolved data acquisition, or signal detection.

#### Excitation by evanescent waves

The concept of this set-up (shown in Fig. 6) is based on total internal reflection fluorescence (TIRF), which has been an established method in fluorescence microscopy and biomedical imaging for more than a decade now [87]. A light beam penetrates an interface between two phases of different refractive index and is totally reflected in the higher refractive index medium, if the angle of incidence exceeds a critical angle. While the light is totally reflected, an electron density wave is generated at the interface to the lower refractive index medium called the evanescent wave. This wave will expand into the medium of lower refractive index, but its strength will decay exponentially. The TIRF system takes advantage of the evanescent wave to specifically illuminate a range not exceeding 100–200 nm from the microscope slide. The penetration depth is a function of refractive index difference, wavelength, incident angle, and thickness of the high refractive index layer.

The high refractive index medium can be a microarray glass slide or a polymer substrate. A single DNA sensor chip was first built up from a PMMA prism for the detection of PCR products [88]. Several approaches have been presented for the analysis of DNA or protein microarrays, including single or multiple total internal reflection at glass substrates [89, 90], or the use of microarray substrates coated with a planar waveguide layer with a high refractive index like Ta<sub>2</sub>O<sub>5</sub> [91, 92]. The latter creates an evanescent field strength several times stronger than that of a glass slide. In this case, the excitation light beam is expanded in one dimension with the help of a cylindrical lens. The light is then coupled into the planar waveguide layer by a diffraction grating incorporated into the chip surface. The main advantage of this system is the superior background elimination, as only the fluorophores that are located immediately at the interface are excited. The chips can be applied in a microfluidic device, enabling the real-time monitoring of binding events on the surface without washing or rinsing steps. The detection limit was found to be as low as 0.8 zmol of Cy5-labeled antibody per microspot.

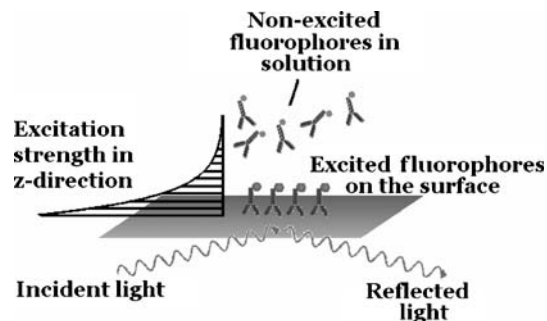


Fig. 6 Principle of total internal reflection fluorescence (TIRF) applied on microarrays

#### Fluorescence anisotropy

Due to their unsymmetric structure, fluorophores produce an anisotropy in the emitted light. The fluorescence anisotropy is defined as the excess value along a particular axis, as

$$r = \frac{I_{\parallel} - I_{\perp}}{I_{\parallel} + 2I_{\perp}}$$

where  $I_{\parallel}$  and  $I_{\perp}$  are the fluorescence intensities parallel and perpendicular to that direction, respectively. Numerous homogenous assays are reported which are based on changes in fluorescence polarization due to biomolecular interactions. They can also be applied in high-throughput screening approaches [93–95]. In solution, the rotational diffusion is rapid, and the emitted light is quickly depolarized. If bound to the solid phase, the fluorophore can be trapped at a certain orientation, and the resulting emission will be strongly anisotropic. The amount of polarization anisotropy is dependent on the amount of labeled biomolecules bound to the surface. On the other hand, fluorescently labeled probes like aptamers can be immobilized on the microarray surface for protein detection [96]. Aptamer–protein interactions can be detected by changes of the fluorescence polarization, collecting the intensities for the parallel and the perpendicular component simultaneously. In this approach, a TIRF set-up was equipped with a polarizing beam splitter. The advantage this approach offers is that the probe molecules are fluorescently labeled, so that the target proteins need no staining or labeling, nor incubation with labeled antibodies for their detection. The design of labels which are appropriate for polarization assays is still an active area of research [97].

#### Time-resolved fluorescence

The fluorescence lifetime  $\tau$  is defined as the time after which the possibility that a fluorophore is still in the excited state has dropped to  $1/e$ . It can be expressed as the inverse sum of radiative and non-radiative rate constants. Basic principles and applications of time-resolved fluores-

cence spectroscopy and fluorescence lifetime imaging microscopy (FLIM) are discussed elsewhere in numerous publications [98–101]. The easiest way to perform FLIM consists in triggering a pulsed light source synchronized with a gated detector (e.g., a CCD camera) with the help of a digital pulse generator. Time-domain measurements very quickly reveal basic parameters like luminescence lifetimes of the selected dyes and their spatially resolved distribution in a sample [102]. Frequency-domain FLIM needs a continuous-wave laser as light source, usually coupled to an acousto-optical modulator [103], but the development of directly modulated light sources is making fast progress. The phase shifts and modulation ratios are measured relative to a fluorescence standard and the lifetime can be rapidly calculated from these parameters.

Lifetime imaging of sensor arrays is usually carried out in the time domain [104]. Digital gated image intensifier detector modules (ICCDs) can now operate at the picosecond level. Figure 7 illustrates different methods for time-resolved data acquisition.

Like steady-state intensity imaging, time-resolved gated imaging (Fig. 7a) has one detection window only. As the image is collected after a certain time delay, fast-decaying background fluorescence can be eliminated. Lifetimes of typical organic fluorescent labels are between 0.5 and 5 ns, whereas autofluorescence from microarray substrates and most biological samples decay in the picosecond range. The ratiometric methods of phase delay rationing (PDR, Fig. 7b) and rapid lifetime determination (RLD, Fig. 7c) [105] offer some more distinct advantages besides background elimination: (a) fluorescence lifetime and its change as additional analytical parameters; (b) independency of intensity fluctuations of the light source or inhomogeneities in the light field; (c) lower sensitivity to the local fluorophore concentration and photobleaching; and (d) elimination of light scatter effects. Therefore, a higher spot homogeneity can be generated by means of these internally referenced methods. Assuming a single exponential decay of the emitted fluorescence with an amplitude  $\alpha$  after a short excitation pulse, the time gated intensity  $I$  is given by

$$I = \int_t^{t+\Delta t} \alpha \exp(-t/\tau) dt$$

In lifetime imaging, fluorescence is detected at various delay times with adjustable time gates  $\Delta t$  in consecutive acquisition cycles (multigate detection). In the case of a monoexponential decay and an identical adjustment of  $\Delta t$ , the lifetime  $\tau$  can be calculated from four experimental parameters:

$$\tau = \frac{t_2 - t_1}{\ln(I_1/I_2)}$$

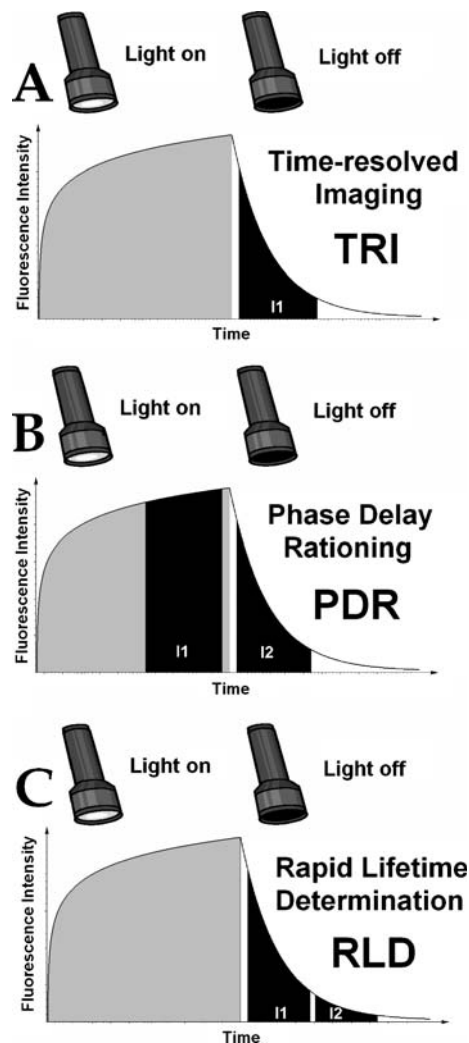


**Fig. 7** Typical time-resolved fluorescence imaging and lifetime imaging modes.  $I_1$  and  $I_2$  represent the time windows with opened detector (CCD camera)

In the case of a multi-exponentially decaying lumino-phore this equation gives only an approximate value of the average decay time.

In practice, the images of the two different gates are taken usually separately in subsequent acquisition cycles. The evaluation software integrates the two sets of pictures, followed by a subtraction of the corresponding background dark pictures (detected with the same time gates and frequency but without illumination). Figure 8 illustrates the whole process for RLD imaging where four sets of images are obtained and integrated: image 1 ( $I_1$ ), image 2 ( $I_2$ ), dark image 1 ( $D_1$ ), and dark image 2 ( $D_2$ ). The ratio  $R$  is calculated according to:

$$R = \frac{\sum I_1 - \sum D_1}{\sum I_2 - \sum D_2}$$

CCD cameras equipped with a multichannel-plate image intensifier can be operated at internal frequencies of up to 12.5 MHz with a time-resolution (minimal gate width) of 3 ns. This is of course insufficient for very rapidly decaying labels. Faster CCD detectors can be obtained with a microchannel plate photomultiplier, working with gating rates of around 100 MHz and a time-resolution of 20 ps, which matches the decay profiles of the commonly used organic fluorescent markers. These camera systems are comparatively expensive and require highly sophisticated accessories for short pulsed excitation, synchronization, and data acquisition. Usually, high gating frequencies are accompanied by a high background noise.

In a first approach using lifetime imaging for DNA microarray analysis, the near-infrared dyes Al-naphthalocyanine ( $\tau=2.7$  ns) and IRD800 ( $\tau=0.8$  ns) were applied on a custom confocal fluorescence lifetime microscope with a pumped laser diode as the excitation source [106]. As most photomultipliers show a poor quantum efficiency in the IR region, the authors used a single photon avalanche diode (SPAD) as detector. They found that the signal-to-noise ratio increased by a factor of 10 when lifetime contrast was added.

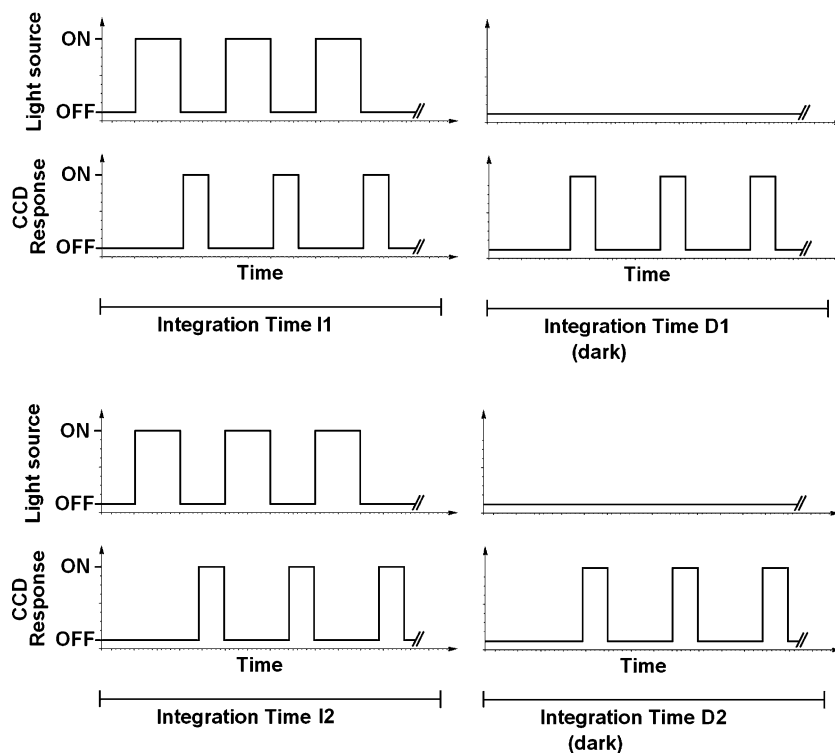
Cubeddu et al. have contemporaneously developed an experimental set-up with a fast light intensifier coupled CCD camera (minimum gate 300 ps) and a dye laser, pumped by either an argon ion or a second-harmonic mode-locked Nd:YLF laser as the excitation source for time-resolved imaging of DNA arrays [107]. Two types of experiments were conducted in a  $10 \times 10$  spot matrix: mutation DNA arrays with targets modified by a single marker (Cy3) and cDNA arrays for expression profiling using target mixtures bearing two different dyes, employ-

ing concentrations of target oligonucleotides as low as 500 pM. They used 44 images delayed by 250 ps to each other to calculate the lifetime on each pixel and while the arrays taken in the intensity mode were barely visible on their apparatus at this concentration, they obtained an increase in SNR of 2.5 and a clear mismatch discrimination upon adding lifetime information onto the images. However, this imaging set-up is composed of rather expensive and complex units like an intensified CCD camera and mode-locked lasers.

A favorable alternative is offered by CCD systems with an electronic (or mechanical) shutter. These achieve internal frequencies of typically 100 kHz and a minimal gating time down to 10–100 ns. These systems require fluorescent labels with decay times preferentially higher than 100 ns. Lanthanide complexes like europium or terbium chelates are extensively used for time-resolved fluoroimmunoassays. They exhibit decay times in the  $\mu$ s range and can be functionalized with amino- [108] or thiol-reactive groups [109] for the attachment to proteins. Naturally, lanthanide chelates can also be used for the labeling of DNA [110]. The suitability of lanthanide tags for time-resolved microarray imaging was demonstrated on a small  $3 \times 3$  protein array under a fluorescence microscope [108]. On the other hand, monofunctional *p*-isothiocyanatophenyl derivatives of platinum(II) coproporphyrin-I have been evaluated as phosphorescent labeling reagents for DNA hybridization assays [111], and protein [112] or antibody detection [113]. The third species of labels with  $\mu$ s lifetimes are ruthenium complexes with bipyridyl- and phenanthroline-derived ligands [114].

To achieve better brightness, these long-lived fluorophores can be incorporated into polymer nanoparticles as

**Fig. 8** Data acquisition process for ratiometric fluorescence lifetime imaging according to the rapid lifetime determination method



described above. For example, platinum tetrapentafluorophenylporphyrin, which has a lifetime of approximately 100  $\mu\text{s}$ , can be applied in poly(acrylic acid)-based copolymers. These nanobeads can be used as labels for protein microarrays via streptavidin coupling on the particle surface. The long lifetime and the huge Stokes shift enables the use of an array of commercial, low-cost 405-nm LEDs as the light source and low-end optical filters. Time-resolved detection was accomplished using a modulated CCD camera in a straightforward set-up illustrated in Fig. 9. From the time-resolved experiments it was clearly evident that adding lifetime information decreases the noise caused by unspecific absorption of the particles and increases the limit of detection [9].

Despite the merits of time-resolved methods like good spot homogeneity, low background and high signal-to-noise ratios, they have not found their way into commercial microarray read out methods. As shown, more straightforward devices can be achieved by application of metal complex labels with high luminescent lifetimes. In analogy to fluorescence polarization (see the last section), the lifetime of a probe label can change significantly after a biomolecular recognition with a target molecule. By using two labels with different decay times new opportunities for internal referencing or differential expression profiling can be seized. This could enable a dual luminophore screening of microarrays in a single detection cycle, if the labels can be excited at the same wavelength and show different lifetimes, in analogy to the time domain dual lifetime referencing method [115].

### Resonance energy transfer assays

The non-radiative transfer of excitation energy requires a spectral overlap between a donor and an acceptor molecule and can be used for the detection of biomolecular interactions like DNA hybridization, antigen–antibody binding, or ligand–receptor recognition. It occurs if the emission spectrum of the donor partially coincides with the absorption spectrum of the acceptor. Such transitions are in

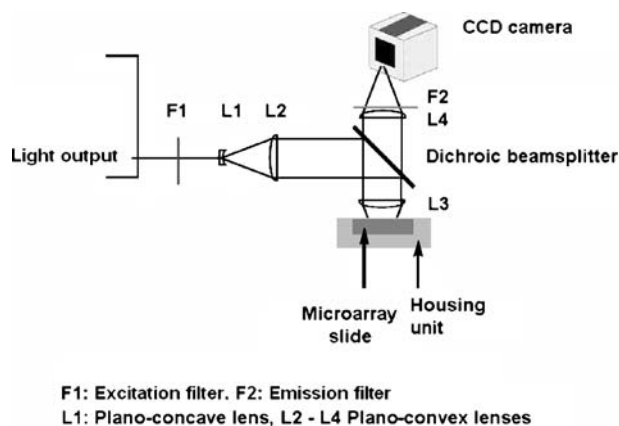


**Fig. 9** Exemplary experimental set-up of a fluorescence lifetime imaging system suitable for the read out of microarrays

resonance, so the term Förster resonance energy transfer (FRET) is often used in the literature [98]. Many luminescent donor–acceptor pairs are well established [116]. Biomolecular recognition forces the donor–acceptor couple into close spacial proximity (Fig. 10), and the resulting energy transfer can be detected via the quenching of the fluorescence of the donor or the specific emission of the acceptor dye if the donor is excited. Förster resonance energy transfer takes place over a distance of around 1–10 nm between donor and acceptor and results from long-range dipole–dipole interactions.

Up to now, the detection of biomolecular interactions by FRET has only found limited applications in the DNA or protein array sector, although its use is attractive because it can confirm interactions on the molecular level with high sensitivity. Such assays can be applied as ratiometric methods by screening the donor and acceptor fluorescence at different wavelengths. A FRET-based technique for SNP detection on DNA microarrays was demonstrated by Frutos et al. [117] who immobilized oligonucleotides labeled with the donor Cy3, on which they subsequently incubated complementary probes labeled with the FRET acceptor carboxy-x-rhodamine. The probes contained a mismatch, and in a competitive assay the Cy3-fluorescence increased after addition of a perfectly matching sequence. This approach is related to the molecular beacon concept. In this case, the immobilized DNA probe has complementary ends and forms a stem-and-loop structure. Both fluorophore and quencher are linked to the two ends of the stem. This non-fluorescent structure becomes fluorescent if the loop hybridizes with its target and the conformational reorganization into a rigid double helix separates the quencher from the fluorophore [118].

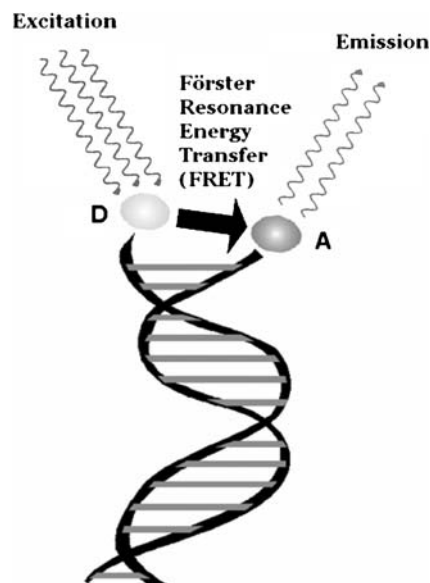


**Fig. 10** Illustration of resonance energy transfer. Specific interactions of biomolecules implicate a close proximity (<10 nm is required for an effective Förster transfer) of a fluorescent donor (D) and an acceptor (A), which acts as the emitter

Time-resolved (TR) FRET assays are known to be very sensitive, e.g., for detection of DNA hybridization [119] or for competitive protein recognition assays [33]. Recently, TR-FRET was applied to protein microarray analysis [9]. The array contained spots of equal concentrations of biotinylated bovine serum albumin (BSA), which was additionally labeled with a long-lived reactive platinum–coproporphyrin-derived compound ( $\tau \approx 100 \mu\text{s}$ ), serving as FRET donor. Then the spots were incubated with different concentrations of streptavidin, labeled with the short-lived FRET acceptor Cy5 ( $\tau \approx 3 \text{ ns}$ ). FRET to Cy5 resulted in a decrease in lifetime due to the shift of emission from the platinum porphyrin to Cy5. Furthermore, it could be demonstrated that t-DLR, which takes the ratio of one image inside and one or two images outside the excitation phase employing a short delay after the end of the light pulse, is also useful for imaging FRET assays. In the image recorded inside the excitation period both dyes are visible; however, because of the delay, the shorter-lived emission is absent in the images recorded after the light pulse. The ratio of these two images is directly related to the ratio of the two dyes, and, in this case, it gives information about the extent of FRET.

### Non-fluorescent methods

In the emerging field of proteomics, analytical methods like 2D gel electrophoresis, with a read out usually based on imaging, and non-imaging methods like mass spectrometry (MS) or surface plasmon resonance (SPR) are complementing one another. Non-imaging methods have evoked great interest in the screening of biomolecular interactions in recent years, because they are label-free techniques and they reveal additional information about the nature of the bound target molecule (MS) or the kinetics of the binding process (SPR). MS modes like MALDI-TOF can easily be combined with microarray formats which have an ionizable conducting surface like gold or aluminium. Ready-for-use protein array chips for MALDI-TOF instruments are marketed, e.g., such as the SELDI Protein Chip (surface enhanced laser desorption ionization) [120]. However, for high-throughput screening applications, MS on high density arrays is too complex and time-consuming. In this section, some non-fluorescent evaluation methods will be highlighted, which cover current improvements of label-free detection techniques like ellipsometry and surface plasmon microscopy. It should also be noted that screening with radioactive labeled ligands or radioimmunoassays is still of interest. Some laser scanner instruments are additionally equipped with a phosphorimaging plate, exhibiting higher sensitivity, dynamic range (five orders of magnitude), and spatial resolution (pixel size down to  $25 \mu\text{m}$ ) than X-ray films. Such plates are reusable 2D sensors for the detection and storage of ionizing radiation. The principle of photostimulated luminescence is used for detection here [121]. A comprehensive discussion on radioisotope labeling and the corresponding imaging methods is beyond the scope of this review.

### Imaging ellipsometry

Ellipsometry is a non-destructive and label-free optical method for determining the thickness of thin films and optical properties of surface layers. The principle of the measurement is based on the change of the polarization of light reflected by the surface coating (Fig. 11). The relative phase shift  $\Delta$  and the change of the ellipsometric angle  $\Psi$  (the ratio of amplitude changes for the respective polarization components  $E_p$  and  $E_s$ ) of a linearly polarized laser beam compared to the blank substrate is detected by an analyzer. When linear polarized light interacts with different kinds of surface modifications, its parallel and perpendicular components are reflected from the surface in a different way. Consequently, the amplitude and phase of both components are changed, resulting in an elliptically polarized light. From these parameters the refractive index and the thickness of the surface coating can be deduced [122]. The laser beam hits the surface at an angle of incidence usually around  $60^\circ$ – $70^\circ$  (relative to the surface normal). The resolution for the determination of a film thickness is below  $1 \text{ \AA}$ , thus the immobilization of biomolecules like proteins or DNA on surface monolayers can easily be observed. Note that “imaging ellipsometry” is a fixed but somewhat misleading term, as it is a scanning and not an imaging method (see also definitions in the section “Laser scanner versus imaging instruments”).

In imaging ellipsometry the surface of a microarray can be scanned by the laser beam with an x/y-resolution of approximately  $1 \mu\text{m}$ . The polarization analyzer is combined with a CCD camera and ellipsometric contrast images can be generated, visualizing the thickness of a surface coating in relation to the blank area around the spots. A general problem of imaging ellipsometry is the inclined observation angle. Thus, only a limited area of the image appears to be well-focused when using conventional optics. This limitation is overcome by using a motorized focusing mechanism to collect a series of images with different foci within the field-of-view. A digital image processing system then superimposes only the focused parts of an image series. For the principle of imaging null ellipsometry the reader should consult the manufacturer’s information brochures [123].

Although this method is principally suited for high-throughput screening of microarray-based assays [124–

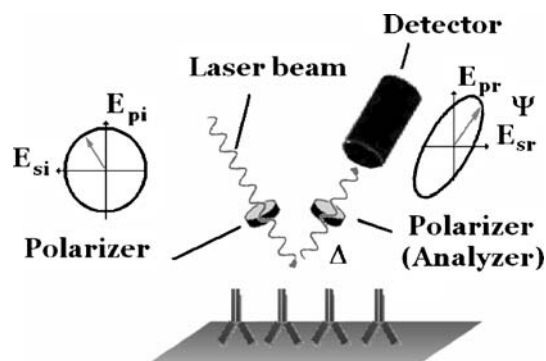


Fig. 11 Principle of ellipsometric surface analysis

[126], it is preferentially used for microarray development, quality control purposes, and the characterization of monolayer properties. Lithographic processes, regularity of surface patterns, spot morphologies, and packing densities of immobilized biomolecular probes can be controlled by means of this ellipsometric “height” imaging [127–130].

### Surface plasmon microscopy

Surface plasmon resonance (SPR) is another label-free technology for monitoring biomolecular interactions with high sensitivity in a real-time mode. Thus, additional information on kinetics and binding constants can be deduced from SPR data. Surface plasmon polaritons are electromagnetic modes propagating along a metal–dielectric interface. Excitation of surface plasmons by photons requires plasmon coupling devices like prisms. In the Kretschmann configuration, the prism is coated with a thin metal layer (gold or silver) [122]. A laser beam is coupled to the plasmon surface polariton modes at the metal–coating–air interface via a right-angle glass prism in an attenuated total reflection geometry [131]. Under certain conditions, depending on the angle of incident light and its wavelength, the surface plasmons get in resonance with the light. As a result of this resonance, the reflection of light decreases to a minimum. Because the resonance conditions also depend on the dielectric coefficient of the adjacent layer, any thin dielectric coating on the metal surface causes an angular shift of the resonance, and therefore a shift of the plasmon resonance minimum of the reflected light can be observed. Only p-polarized light that is in the plane of incidence with the electric field vector oscillating perpendicular to the plane of the metal film can couple to the plasmon polaritons. S-polarized light with an electric field vector orientated parallel to the metal film cannot excite plasmons, but is reflected by the metal surface and can be used as reference signal. For biochemical sensors, the detection of the shift of the resonance angle at a fixed wavelength has become the method of choice. As interactions with surface-bound probes like single-stranded DNA, receptors, or antibodies can be monitored in situ and without labeling, SPR devices are of great interest in biotechnology research and pharmaceutical screening.

Surface plasmon microscopy (SPM), or alternatively called SPR imaging, was introduced by Rothenhäusler and Knoll, using a CCD camera as the detector (Fig. 12) [132]. A parallel beam of monochromatic light is coupled to the surface plasmon with one certain angle of incidence. The reflected light is focused by a lens and recorded by means of the CCD camera. A polarizer separates p- and s-polarized light and the latter is used as reference. A patterned dielectric layer, e.g., a protein array, on the metal film causes different resonance angles. As in this case the angle of incident light is fixed, the reflected intensity will be changed, leading to a contrast image of the surface. Contrast enhancement can be achieved by dark-field imaging [133] or by SPR interferometry [134, 135].

Another approach is based on the combination of ellipsometry and SPR, at which the SPR cell and geometry is integrated in an imaging ellipsometer as described above. In this case, the ellipsometrical parameters  $\Delta$  and  $\Psi$  are derived by applying an evanescent field.

The optical set-up requires special instrumentation distinct from the imaging and laser scanner systems presented in “Laser scanner versus imaging instruments”, with a market clearly dominated by the Biacore systems [136]. The sensor chip can be applied in flow-through cells or combined with microfluidic devices, enabling multiplexed thermodynamic and kinetic measurements and the determination of affinity constants. SPM and interferometry provide not only a well-suited method for the quality control of monolayer or multilayer coatings and general surface and patterning properties [137–139], but are also useful for affinity assay development like monitoring DNA hybridizations, SNPs, and protein interactions [140–145]. The sensitivity of SPM systems is very high, e.g., concentrations of 2 nM of RNA could be detected [140]. The multiplexity of such arrays is not very high: densities in the magnitude of 100 spots per chip have been reported. Even enzymatic reactions can be monitored on chip, e.g., phosphorylation reactions by kinase A [146]. The sensitivity of SPM of immunoassays on protein microarray formats can be enhanced by peroxidase-catalyzed precipitation reactions [147].

An SPR multichannel device with specially designed prisms for wavelength division represents a different approach to obtain spatially resolved information [148]. Besides the limited spatial resolution provided by the optical set-up, the SPR multichannel measurements are only applicable for low density array formats with a limited number of spots (e.g., a 4×4 matrix) because of the large amount of data which is produced.

### Conclusion and outlook

This review gives an overall impression of the variety of optical imaging techniques targeted at DNA or protein microarray analysis. The high-throughput read out of such so-called biochips, which is usually accomplished by fluorescence scanning or imaging methods, is of major

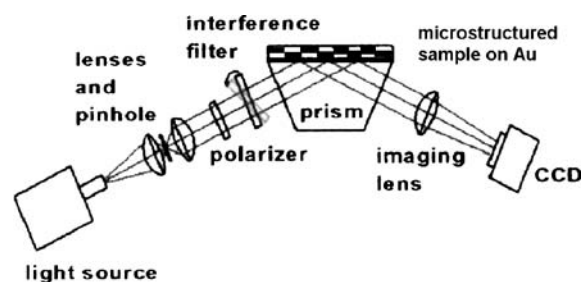


Fig. 12 Schematic of a surface plasmon microscope set-up according to ref. [158]. Other configurations make use of a mirror mounted on a motor-controlled rotation stage for creating parallel beams at fixed position [159]

importance in this field. Recent developments in signal amplification and detector technologies have been illustrated. Further progress can be expected with respect to highly sensitive detector arrays like electron-multiplying CCD chips or multichannel single-photon counting modules. Advanced fluorescent read out methods including TIRF or time-resolved imaging have been highlighted, too. Only time will tell whether they will find special applications and successfully make an impact on the market.

Another challenge for optical imaging methods is the quality control of the biofunctionalized microarray. Non-fluorescent techniques like imaging ellipsometry or SPM can make a useful contribution to this end. These provide the characterization of the surface properties and the patterning of a microarray. Preparation steps as well as the density of immobilized biomolecules can be controlled. Furthermore, biomolecular interactions can be monitored with SPM without labeling and in real-time albeit with a limited degree of multiplexity up to now. Fourier transform infrared spectroscopy (FTIR) imaging is an emerging method for the chemical analysis of surface coatings like self-assembled monolayers, thin polymer films, and protein patterns particularly suited for R&D and quality control purposes.

It should be noted that non-optical imaging techniques like scanning probe microscopy also are very useful as quality control instruments. Among these techniques, atomic force microscopy (AFM) can particularly assist in the characterization of microarray surfaces, because it can image both conducting and nonconducting surface coatings with atomic resolution [149]. The uniformity of binding matrices like SAMs spread on the surface can be visualized by means of AFM, as well as the topology of surfaces patterned with oligonucleotide probes [150] and the binding of single protein molecules [151].

The current trend indicates that microarrays loaded with whole living cells are becoming increasingly important for pharmaceutical drug screening [152], e.g., with respect to cancer therapy [153], and functional genomic [154] or expression studies [155]. Besides pharmaceutical research, cell-based microarrays can also be applied for environmental monitoring and detection of pollutants [156] and genotoxins [157]. In cellular screening, expression constructs with GFP or bioluminescent systems are mostly used as reporter elements, which can be read out by common fluorescent imaging systems and microscopes, if sub-cellular resolution is required. Metabolic imaging is another challenging perspective in connection with cellular microarrays. The indication of regions with increased metabolic rate, such as in tumorous or infected tissue is a valuable tool for monitoring the effectiveness of chemotherapeutic or anti-inflammatory agents. In this case, the changes in relevant intracellular and extracellular parameters like in pH, oxygen partial pressure, and of concentrations of  $\text{Ca}^{2+}$ , glucose, or lactate have to be imaged spatially resolved, while the living tissue is exposed to the therapeutic candidates. A great challenge would be the simultaneous detection of several of these

parameters on one microarray format. New demands for fluorescent imaging systems will arise here with respect to online monitoring, as in this case fluorophores are not used as labels, but as indicators.

## References

1. McCall GH, Barone AD, Diggelmann M, Fodor SPA, Gentalen E, Ngo N (1997) *J Am Chem Soc* 119:5081–5090
2. Pirrung MC (2002) *Angew Chem Int Ed* 41:1276–1289
3. Schäferling M, Kambhampati D (2004) Protein microarray surface chemistry and coupling schemes. In: Kambhampati D (ed) *Protein microarray technology*. Wiley-VCH, Weinheim, pp 11–38
4. <http://www.affymetrix.com>
5. Zhu H, Bilgin M, Bangham R, Hall D, Casamayor A, Bertone P, Lan M, Jansen R, Bidlingmaier S, Houfek T, Mitchell T, Miller P, Dean RA, Gerstein M, Snyder M (2001) *Science* 293:2101–2105
6. <http://www.invitrogen.com>
7. Haugland RP (2002) *Handbook of fluorescent probes and research products*. Molecular Probes Inc, see: <http://www.probes.com>
8. <http://www.amershambiosciences.com>
9. Nagl S, Schäferling M, Wolfbeis OS (2005) *Microchim Acta* 151:1–21
10. Rolfs A, Sculler I, Finckh U, Weber-Rolfs I (1992) *PCR: clinical diagnostic and research*. Springer, Berlin Heidelberg New York
11. Saiki RK, Scharf S, Faloona F, Mullis KB, Horn GT, Erlich HA, Arnheim N (1985) *Science* 230:1350–1354
12. Dirks RW, Van Gijlswijk RPM, Vooijs MA, Smit AB, Bogerd J, Van Minnen J, Raap AK, Van der Ploeg M (1991) *Exp Cell Res* 194:310–315
13. Templin MF, Stoll D, Schwenk JM, Pötz O, Kramer S, Joos TO (2003) *Proteomics* 3:2155–2166; MacBeath G (2002) *Nature Gen Suppl* 32:526–532; Kumble KD (2003) *Anal Bioanal Chem* 377:812–819; Espina V, Mehta AI, Winters ME, Calvert V, Wulfkuhle J, Petricoin III EF, Liotta LA (2003) *Proteomics* 3:2091–2100
14. Schena M (ed) (2004) *Protein microarrays*. Jones and Bartlett, Boston; Albala JS, Humphery-Smith I (eds) (2003) *Protein arrays. Biochips and proteomics*. Marcel Dekker, New York; Fung E (ed) (2004) *Protein arrays: methods and protocols (Methods in molecular biology)*. Humana Press, Totowa; Joos TO, Fortina P (eds) (2005) *Microarrays in clinical diagnostics*. Humana Press, Totowa
15. Seong S, Choi C (2003) *Proteomics* 3:2176–2189
16. Fang Y (2004) Universal readout for target identification using biological microarrays. US 2004185445 A1 20040923; Scorilas A, Bjartell A, Lilja H, Moller C, Diamandis EP (2000) *Clin Chem* 46:1450–1455
17. Wiese R (2003) *Luminescence* 18:25–30
18. Wilson WJ, Stout CL, DeSantis TZ, Stilwell JL, Carrana AV, Andersen GL (2002) *Mol Cell Probes* 16:119–127
19. Song JY, Park HG, Jung SO, Park JC (2005) *Nucleic Acids Res* 33:e19
20. Kukar T, Eckenrode S, Gu Y, Lian W, Megginson M, She JX, Wu D (2002) *Anal Biochem* 306:50–54
21. Coleman MA, Lao VH, Segelke BW, Beernik PT (2004) *J Prot Res* 3:1024–1032
22. Choi YS, Pack SP, Yoo YJ (2005) *Biochem Biophys Res Comm* 329:1315–1319
23. Berlier JE, Rothe A, Buller G, Bradford J, Gray DR, Filanoski BJ, Telford WG, Yue S, Liu J, Cheung C-Y, Chang W, Hirsch JD, Beechem JM, Haugland RP, Haugland RP (2003) *J Histochem Cytochem* 51:1699–1712
24. Madison R, Macklis JD, Thies C (1990) *Brain Res* 522:90–98
25. Panyam J, Sahoo SK, Prabha S, Bargar T, Labhasetwar V (2003) *Int J Pharm* 23:1–11



26. Härmä H, Pelkkikangas A-M, Soukka T, Huhtinen P, Huopalahti S, Lövgren M (2003) *Anal Chim Acta* 482:157–164
27. Guo CY, Shankar RR, Abe S, Ye Z, Thomas RN, Kuo JE (1992) *Anal Biochem* 207:241–248
28. Jaulin N, Appel M, Passirani C, Barratt G, Labarre D (2000) *J Drug Target* 8:165–172
29. Kürner JM, Klimant I, Krause C, Preu H, Kunz W, Wolfbeis OS (2001) *Bioconj Chem* 12:883–889
30. Taniguchi H, Nishiya M, Tanosaki S, Inaba H (1996) *Optics Lett* 21:263–265
31. Li Z, Liu G, Law S-J, Sells T (2002) *Biomacromolecules* 3:984–990
32. Cao Y, Koo Y-EL, Kopelman R (2004) *Analyst* 129:745–750
33. Kürner JM, Wolfbeis OS, Klimant I (2002) *Anal Chem* 74:2151–2156
34. Lian W, Litherland SA, Badrane H, Tan W, Wu D, Baker HV, Gulig PA, Lim DV, Jin S (2004) *Anal Biochem* 334:135–144
35. Santra S, Zhang P, Wang K, Tapeç R, Tan W (2001) *Anal Chem* 73:4988–4993
36. Santra S, Yang D, Dutta D, Stanley JT, Holloway PH, Tan W, Moudgil BM, Mericle AR (2004) *Chem Commun* 24:2810–2812
37. Tan M, Ye Z, Wang G, Yuan J (2004) *Chem Mater* 16:2494–2498
38. Ye Z, Tan M, Yuan J (2004) *Anal Chem* 76:513–518
39. Alivisatos P (2004) *Nat Biotechnol* 22:47–52
40. Smith AM, Nie S (2004) *Analyst* 129:672–677
41. Michalet X, Pinaud FF, Bentolila LA, Tsay JM, Doose S, Li JJ, Sundaresan G, Wu AM, Gambhir SS, Weiss S (2005) *Science* 307:538–544
42. <http://www.qdots.com>
43. Gao X, Nie S (2004) *Nanobiotechnology* 324–352
44. Chan WCW, Maxwell DJ, Gao X, Bailey RE, Han M, Nie S (2002) *Curr Opin Biotechnol* 13:40–46
45. Gao X, Yuanyuan C, Levenson RM, Chung LWK, Nie S (2004) *Nature Biotechnol* 22:969–976
46. Gao X, Yang L, Petros JA, Marshall FF, Simons JW, Nie S (2005) *Curr Opin Biotechnol* 16:63–72
47. Medintz IL, Uyeda HT, Goldman ER, Mattoussi H (2005) *Nat Mater* 4:435–446
48. Gerion D, Chen F, Kannan B, Fu A, Parak WJ, Chen DJ, Majumdar A, Alivisatos AP (2003) *Anal Chem* 75:4766–4772
49. Liang RQ, Li W, Li Y, Tan CY, Li JX, Jin YX, Ruan KQ (2005) *Nucl Acids Res* 33:e17
50. Goldman ER, O'Shaughnessy TJ, Soto CM, Patterson CH Jr, Taitt CR, Spector MS, Charles PT (2004) *Anal Bioanal Chem* 380:880–886
51. Geho D, Lahar N, Gurnani P, Huebschman M, Herrmann P, Espina V, Shi A, Wulfschuhle J, Garner H, Petricoin E III, Liotta LA, Rosenblatt KP (2005) *Bioconj Chem* 16:559–566
52. Schweitzer B, Kingsmore S (2001) *Curr Opin Biotech* 12:21–27
53. Nallur G, Luo C, Fang L, Cooley S, Dave V, Lambert J, Kukanskis K, Kingsmore S, Lasken R, Schweitzer B (2001) *Nucleic Acids Res* 29:e118
54. Kashkin KN, Strizhkov BN, Gryadunov DA, Surzhikov SA, Grechishnikova IV, Kreindlin EY, Chupeeva VV, Evseev KB, Turygin AY, Mirzabekov AD (2005) *Mol Biol* 39:26–34
55. Favis R, Day J, Gerry N, Phelan C, Narod C, Barany F (2000) *Nat Biotechnol* 18:561–564
56. Hall EAH (1991) *Biosensors*. Open University Press, Oxford
57. <http://www.promega.com>
58. Mendoza LG, McQuary P, Mongan A, Gangadharan R, Brignac S, Eggers M (1999) *BioTechniques* 27:778–788
59. Wiese R, Belosludtsev Y, Powderill T, Thompson P, Hogan M (2001) *Clin Chem* 47:1451–1457
60. Avseenko NV, Morozova TY, Ataullakhanov FI, Morozov VN (2002) *Anal Chem* 74:927–933; David CA, Middleton T, Montgomery D, Lim HB, Kati W, Molla A, Xuel X, Warrior U, Kofron JL, Burns DJ (2002) *J Biomol Screen* 7:259–266
61. Joos TO, Schrenk M, Höpfl P, Kröger K, Chowdhury U, Stoll D, Schörner D, Dürr M, Herick K, Rupp S, Sohn K, Hämmerle H (2000) *Electrophoresis* 21:2641–2650
62. Huang RP, Huang R, Fan Y, Lin Y (2001) *Anal Biochem* 294:55–62
63. Knecht BG, Strasser A, Dietrich R, Märklbauer E, Niessner R, Weller MG (2004) *Anal Chem* 76:646–654
64. Bacarese-Hamilton T, Mezzasoma L, Ingham C, Ardizzoni A, Rossi R, Bistoni F, Frisanti A (2002) *Clin Chem* 48:1367–1370
65. Woodbury RL, Varnum SM, Ranger RC (2002) *J Prot Res* 1:233–237
66. Baggerly K, Mitra R, Grier R, Medhane D, Lozano G, Kapoor M (2004) *Anal Chim Acta* 506:117–125
67. Richter A, Schwager C, Hentze S, Ansorge W, Hentze MW, Muckenthaler M (2002) *BioTechniques* 33:620–628
68. Wiltshire S, O'Malley S, Lambert J, Kukanskis K, Edgar D, Kingsmore SF, Schweitzer B (2000) *Clin Chem* 46:1990–1993
69. Fritzsche W, Taton TA (2003) *Nanotechnology* 14:R63–R73
70. Sauer U, Preininger C, Krumpel G, Stelzer N, Kern W (2005) *Sens Act B* 107:178–183
71. Que W, Sun Z, Chan YL, Kam CH (2000) *Thin Solid Films* 359:177–183
72. Angenendt P, Glökler J, Murphy D, Lehrach H, Cahill DJ (2002) *Anal Biochem* 309:253–260
73. Ramm P (2005) *Curr Opin Biotechnol* 16:41–48
74. Pickett SC (2003) *IVD technology* May:45–50, <http://www.device-link.com/ivdt/archive/03/05/007.html>
75. Cortese JD (2001) *Scientist* 15(24):36
76. White J (2004) *Pharm Discov* 4(8):30–34
77. <http://www.biocompare.com/matrix/931/Microarray-Scanners.html>
78. [http://ihome.cuhk.edu.hk/~b400559/arraysoft\\_image.html](http://ihome.cuhk.edu.hk/~b400559/arraysoft_image.html)
79. Preininger C, Sauer U (2004) Design, quality control and normalization of biosensor chips. In: Narayanaswamy R, Wolfbeis OS (eds) *Springer series on chemical sensors and biosensors, optical sensors, vol 1*. Springer Verlag, Berlin heidelberg New York, pp 67–92
80. Bunes A, Huber W, Steiner K, Sultmann H, Poustka A (2005) *Bioinformatics* 21:554–556
81. Cronin M, Ghosh K, Sistare F, Quackenbush J, Vilker V, O'Connell C (2004) *Clinical Chem* 50:1464–1471
82. (a) Andersen MT, Foy CA (2005) *Anal Bioanal Chem* 381:87–89; (b) <http://www.mged.org/>
83. Janesick J, Putnam G (2003) *Annu Rev Nucl Part Sci* 53:263–300
84. Dautet H, Deschamps P, Dion B, MacGregor AD, MacSween D, McIntyre RS, Trottier C, Webb PP (1993) *Appl Opt* 32:3894–3900
85. Trottier C, Davies M, Dautet H, Wabuyele M, Soper SA, Kapanidis AN, Lacoste T, Weiss S (2004) *Pharma Genomics* 4(2):24–34
86. Rabinovich E, O'Brien MJ, Brueck SRJ, Lopez GP (2000) *Rev Sci Instrum* 71:522–529
87. Axelrod D (2001) *Methods Cell Imaging* 362–380
88. Peter C, Meusel M, Grawe F, Katerkamp A, Cammann K, Borchers T (2001) *Fresenius J Anal Chem* 371:120–127
89. Lehr H-P, Brandenburg A, Sulz G (2003) *Sens Act B* 92:303–314
90. Lehr H-P, Reimann M, Brandenburg A, Sulz G, Klapproth H (2003) *Anal Chem* 75:2414–2420
91. Pawlak M, Schick E, Bopp MA, Schneider MJ, Oroszlan P, Ehrat M (2002) *Proteomics* 2:383–393
92. Duvencek GL, Abel AP, Bopp MA, Kresbach GM, Ehrat M (2002) *Anal Chim Acta* 469:49–61
93. Park S-H, Raines RT (2004) *Meth Mol Biol* 261:161–165
94. Blommel P, Hanson GT, Vogel KW (2004) *J Biomol Screen* 9:294–302
95. Schust J, Berg T (2004) *Anal Biochem* 330:114–118
96. McCauley TG, Hamaguchi N, Stanton M (2003) *Anal Biochem* 319:244–250
97. Dürkop A, Lehmann F, Wolfbeis OS (2002) *Anal Bioanal Chem* 372:688–694
98. Valeur B (2002) *Molecular fluorescence*. Wiley-VCH, Weinheim
99. Wang XF, Periasamy A, Herman B (1992) *Crit Rev Anal Chem* 23:369–395
100. Clegg RM, Holub O, Gohlke C (2003) *Fluorescence lifetime-resolved imaging: measuring lifetimes in an image*. In: *Methods in Enzymology* vol 360, Elsevier Science (USA) 509–542

101. Herman P, Lin HJ, Lakowicz JR (2003) Lifetime-based Imaging. In: Vo-Dinh T (ed) Biomedical photonics handbook. CRC Press Boca Raton, pp 9.1–9.30
102. Wang XF, Herman B (1996) Fluorescence imaging spectroscopy and microscopy. In: Chemical analysis series, vol 137. Wiley, New York
103. Gadella TWJ, Jovin TM, Clegg RM (1993) *Biophys Chem* 48:221–239
104. Schäferling M (2005) Luminescence lifetime-based imaging of sensor arrays for high-throughput screening applications. In: Orellana G, Moreno-Bondi MC (eds) Springer series on chemical sensors and biosensors, frontiers in chemical sensors, vol 3. Springer, Berlin Heidelberg New York (in press)
105. Hartmann P, Ziegler W, Holst G, Lübbers DW (1997) *Sens Actuators B* 38–39:110–115; Woods RJ, Scypinski S, Cline Love LJ (1984) *Ashworth HA, Anal Chem* 56:1395–1400
106. Waddell E, Wang Y, Stryjweski W, McWorther S, Henry AC, Eavns D, McCarley RL, Soper SA (2000) *Anal Chem* 72:5907–5917
107. Cubeddu R, Comelli D, D'Andrea C, Taroni P, Valentini G (2002) *J Phys D Appl Phys* 35:R61–R76
108. Weibel N, Charbonniere LJ, Guardigli M, Roda A, Ziessel R (2004) *J Am Chem Soc* 126:4888–4896
109. Ge P, Selvin PR (2003) *Bioconj Chem* 14:870–876
110. Selvin PR (2003) Lanthanide-labeled DNA. In: Lakowicz JR (ed) Topics in fluorescence spectroscopy, DNA technology, vol 7. Springer, Berlin Heidelberg New York, pp 177–212
111. O'Sullivan PJ, Burke M, Soini A, Papkovsky DB (2002) *Nucl Acids Res* 30:E114
112. O'Riordan TC, Soini AE, Papkovsky DB (2001) *Anal Biochem* 290:366–375
113. O'Riordan TC, Soini AE, Soini JE, Papkovsky DB (2002) *Anal Chem* 74:5845–5850
114. Bannwarth W, Schmidt D, Stallard RL, Hornung C, Knorr R, Mueller F (1988) *Helvetica Chim Acta* 71:2085–2099; Duerkop A, Lehmann F, Wolfbeis OS (2002) *Anal Bioanal Chem* 372:688–694
115. Klimant I, Huber C, Liebsch G, Neurauter G, Stangelmayer A, Wolfbeis OS (2001) Dual lifetime referencing (DLR) - a new scheme for converting fluorescence intensity into a frequency-domain or time-domain information. In: Valeur B, Brochon JC (eds) Springer series in fluorescence spectroscopy, vol 1. Springer, Berlin Heidelberg New York, pp 257–274
116. Selvin PR (2000) *Nat Struct Biol* 7:730–734
117. Frutos AG, Pal S, Quesada M, Lahiri J (2002) *J Am Chem Soc* 124:2396–2397
118. Fang X, Liu X, Schuster S, Tan WJ (1999) *Am Chem Soc* 121:2921–2922
119. Selvin PR (2002) *Annu Rev Biophys Biomol Structure* 31:275–302
120. <http://www.ciphergen.com>
121. <http://home.fujifilm.com/products/science/hardware/bas5000/fea.html>
122. Ulman A (1991) An introduction to ultrathin organic films. Academic Press, San Diego
123. <http://www.nanofilm.de>
124. Vaupel M, Eing A, Greulich K-O, Roegerer J, Schellenberg P, Striebel HM, Arlinghaus HF (2005) Microarray technology and its applications, pp 181–207
125. Bae YM, Oh B-K, Lee W, Lee WH, Choi J-W (2004) *Anal Chem* 76:1799–1803
126. Bae YM, Oh B-K, Lee Wg, Lee WH, Choi JW (2004) *Biosens Bioelectron* 20:895–902
127. Zhou Y, Andersson O, Lindberg P, Liedberg B (2004) *Microchim Acta* 147:21–30
128. Schmaljohann D, Nitschke M, Schulze R, Eing A, Werner C, Eichhorn K-J (2005) *Langmuir* 21:2317–2322
129. Howland MC, Sapuri-Butti AR, Dixit SS, Dattelbaum AM, Shreve AP, Parikh AN (2005) *J Am Chem Soc* 127:6752–6765
130. Wang Z-H, Jin G (2004) *J Immunol Meth* 285:237–243
131. Kretschmann E (1972) *Optics Commun* 6:185–187
132. Rothenhäusler B, Knoll W (1988) *Nature* 332:615–616
133. Grigorenko AN, Beloglazov AA, Nikitin, PI, Kuhne C, Steiner G, Salzer R (2000) *Opt Commun* 174:151–155
134. Nikitin PI, Grigorenko AN, Beloglazov AA, Valeiko MV, Savchuk AI, Savchuk OA, Steiner G, Kuhne C, Huebner A, Salzer R (2000) *Sens Act A* 85:189193; Kabashin AV, Nikitin PI (1997) *Quantum Electronics* 27:653–655
135. Yu X, Wang D, Wie X, Deng Y, Liu J, Ding X (2004) *Chem Sensors* 20:206–207
136. <http://www.biachem.com>
137. Knoll W, Liley M, Piscevic D, Spinke J, Tarlov MJ (1997) *Adv Biophys* 34:231–251
138. Frutos AG, Weibel SC, Corn RM (1999) *Anal Chem* 71:3928–3934
139. Kanda V, Kariuki JK, Harrison DJ, McDermott MT (2004) *Anal Chem* 76:7257–7262
140. Nelson BP, Grimsrud TE, Liles MR, Goodman RM, Corn RM (2001) *Anal Chem* 73:1–7
141. Jordan CE, Frutos AG, Brockmann JM, Corn RM (1997) *Anal Chem* 69:4939–4947
142. Bassil N, Maillart E, Canva M, Levy Y, Millot M-C, Pissard S, Narwa R, Goosens M (2003) *Sens Act B* 313–323
143. Lee HJ, Yan Y, Marriott G, Corn RM (2005) *J Physiol* 563:61–71
144. Jung J-M, Shin Y-B, Kim M-G, Ro H-S, Jung H-T, Chung BH (2004) *Anal Biochem* 330:251–256
145. Yu X, Wang D, Xing W, Ding X, Liao W, Zhao X (2005) *Sens Act B* 108:765–771
146. Inamori K, Kyo M, Nishiya Y, Inoue Y, Sonoda T, Kinoshita E, Koike T, Katayama Y (2005) *Anal Chem* 77:3979–3985
147. Kim M-G, Shin Y-B, Jung J-M, Ro H-S, Chung BH (2005) *J Immun Methods* 297:125–132
148. Dostalek J, Vaisocherova H, Homola J (2005) *Sens Act B* 108:758–764
149. Marti O, Ribi HO, Drake B, Albrecht TR, Quate CF, Hansma PK (1988) *Science* 239:50–52
150. O'Brien JC, Stickney JT, Porter MD (2000) *Langmuir* 16:9559–9567
151. Schäferling M, Kruschina M, Ortigao F, Riepl M, Enander K, Liedberg B (2002) *Langmuir* 18:7016–7023
152. Bailey SN, Wu RZ, Sabatini DM (2002) *Drug Discov Today* 7: S113–S118
153. Henning T, Brischwein M, Baumann W, Ehret R, Freund I, Kammerer R, Lehmann M, Schwinde A, Wolf B (2001) *Anticancer Drugs* 12:21–32
154. Wu RZ, Bailey SN, Sabatini DM (2002) *Trends Cell Biol* 12:485–488
155. Ziauddin J, Sabatini DM (2001) *Nature* 411:107–110
156. Belkin S (2003) *Curr Opin Microbiol* 6:206–212
157. Kuang Y, Biran I, Walt DR (2004) *Anal Chem* 76:2902–2909
158. Fu E, Foley J, Yager P (2003) *Rev Sci Instrum* 74:3182–3184
159. Giebel K-F, Bechinger C, Herminghaus S, Riedel M, Leiderer P, Weiland U, Bastmeyer M (1999) *Biophys J* 76:509–516